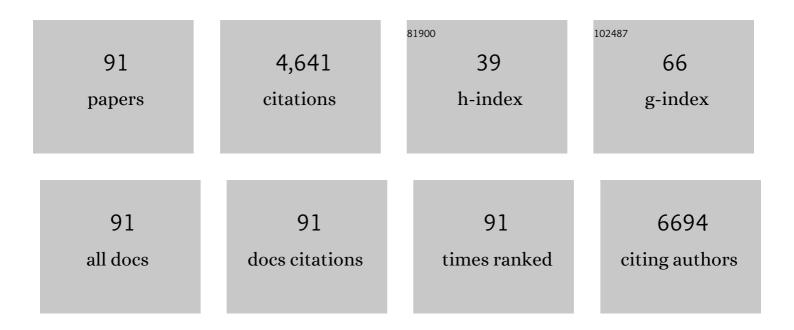


List of Publications by Year in descending order

Source: https://exaly.com/author-pdf/1660691/publications.pdf Version: 2024-02-01



XIA TAO

#	Article	IF	CITATIONS
1	Fabrication of CoTiO ₃ /g-C ₃ N ₄ Hybrid Photocatalysts with Enhanced H ₂ Evolution: Z-Scheme Photocatalytic Mechanism Insight. ACS Applied Materials & Interfaces, 2016, 8, 13879-13889.	8.0	338
2	Enhanced photoelectrocatalytic activity of reduced graphene oxide/TiO2 composite films for dye degradation. Chemical Engineering Journal, 2012, 198-199, 547-554.	12.7	186
3	Defect-rich O-incorporated 1T-MoS2 nanosheets for remarkably enhanced visible-light photocatalytic H2 evolution over CdS: The impact of enriched defects. Applied Catalysis B: Environmental, 2018, 229, 227-236.	20.2	176
4	Novel ZnO-Based Film with Double Light-Scattering Layers as Photoelectrodes for Enhanced Efficiency in Dye-Sensitized Solar Cells. Chemistry of Materials, 2010, 22, 928-934.	6.7	172
5	Fragmented phosphorus-doped graphitic carbon nitride nanoflakes with broad sub-bandgap absorption for highly efficient visible-light photocatalytic hydrogen evolution. Applied Catalysis B: Environmental, 2018, 225, 397-405.	20.2	154
6	One-step hydrothermal synthesis of high-percentage 1T-phase MoS2 quantum dots for remarkably enhanced visible-light-driven photocatalytic H2 evolution. Applied Catalysis B: Environmental, 2019, 243, 76-85.	20.2	137
7	Heteroatoms binary-doped hierarchical porous g-C3N4 nanobelts for remarkably enhanced visible-light-driven hydrogen evolution. Applied Catalysis B: Environmental, 2018, 226, 61-70.	20.2	135
8	Large‣ize, Porous, Ultrathin NiCoP Nanosheets for Efficient Electro/Photocatalytic Water Splitting. Advanced Functional Materials, 2020, 30, 1910830.	14.9	134
9	1T/2H MoSe2-on-MXene heterostructure as bifunctional electrocatalyst for efficient overall water splitting. Electrochimica Acta, 2019, 326, 134976.	5.2	125
10	Mesoporous silica nanotubes coated with multilayered polyelectrolytes for pH-controlled drug release. Acta Biomaterialia, 2010, 6, 3092-3100.	8.3	117
11	Facile Large-Scale Synthesis of Urea-Derived Porous Graphitic Carbon Nitride with Extraordinary Visible-Light Spectrum Photodegradation. Industrial & Engineering Chemistry Research, 2016, 55, 4506-4514.	3.7	116
12	Stable multiphasic 1T/2H MoSe2 nanosheets integrated with 1D sulfide semiconductor for drastically enhanced visible-light photocatalytic hydrogen evolution. Applied Catalysis B: Environmental, 2018, 238, 27-37.	20.2	113
13	lodine-Doped ZnO Nanocrystalline Aggregates for Improved Dye-Sensitized Solar Cells. Chemistry of Materials, 2011, 23, 3-5.	6.7	106
14	Ni ₃ C-Decorated MAPbI ₃ as Visible-Light Photocatalyst for H ₂ Evolution from HI Splitting. ACS Catalysis, 2019, 9, 8144-8152.	11.2	101
15	Nitrogen vacancies modified graphitic carbon nitride: Scalable and one-step fabrication with efficient visible-light-driven hydrogen evolution. Chemical Engineering Journal, 2019, 358, 20-29.	12.7	101
16	Edge-oriented, high-percentage 1T′-phase MoS2 nanosheets stabilize Ti3C2 MXene for efficient electrocatalytic hydrogen evolution. Applied Catalysis B: Environmental, 2021, 284, 119708.	20.2	99
17	Versatility of Carbon Enables All Carbon Based Perovskite Solar Cells to Achieve High Efficiency and High Stability. Advanced Materials, 2018, 30, e1706975.	21.0	95
18	Visible-Light-Responsive TiO ₂ -Coated ZnO:I Nanorod Array Films with Enhanced Photoelectrochemical and Photocatalytic Performance. ACS Applied Materials & Interfaces, 2015, 7, 6093-6101.	8.0	93

#	Article	IF	CITATIONS
19	Efficient, Full Spectrum-Driven H ₂ Evolution Z-Scheme Co ₂ P/CdS Photocatalysts with Co–S Bonds. ACS Applied Materials & Interfaces, 2019, 11, 22297-22306.	8.0	90
20	Nickel-mediated polyol synthesis of hierarchical V ₂ O ₅ hollow microspheres with enhanced lithium storage properties. Journal of Materials Chemistry A, 2015, 3, 1979-1985.	10.3	82
21	Few-layer black phosphorus-on-MAPbI3 for superb visible-light photocatalytic hydrogen evolution from HI splitting. Applied Catalysis B: Environmental, 2019, 259, 118075.	20.2	82
22	Controllable assembly of well-defined monodisperse Au nanoparticles on hierarchical ZnO microspheres for enhanced visible-light-driven photocatalytic and antibacterial activity. Nanoscale, 2015, 7, 19118-19128.	5.6	79
23	Fluorescent mesoporous silica nanotubes incorporating CdS quantum dots for controlled release of ibuprofen. Acta Biomaterialia, 2009, 5, 3488-3496.	8.3	73
24	Visible-light-response iodine-doped titanium dioxide nanocrystals for dye-sensitized solar cells. Journal of Materials Chemistry, 2011, 21, 3877.	6.7	73
25	Highly effective pH-universal removal of tetracycline hydrochloride antibiotics by UiO-66-(COOH)2/GO metal–organic framework composites. Journal of Solid State Chemistry, 2020, 284, 121200.	2.9	70
26	lodine-doped ZnO nanopillar arrays for perovskite solar cells with high efficiency up to 18.24%. Journal of Materials Chemistry A, 2017, 5, 12416-12425.	10.3	69
27	Low temperature synthesis of iodine-doped TiO2 nanocrystallites with enhanced visible-induced photocatalytic activity. Applied Surface Science, 2011, 257, 5046-5051.	6.1	60
28	Comparative study of solid silica nanoparticles and hollow silica nanoparticles for the immobilization of lysozyme. Chemical Engineering Journal, 2008, 137, 38-44.	12.7	59
29	High-efficiency near-infrared enabled planar perovskite solar cells by embedding upconversion nanocrystals. Nanoscale, 2017, 9, 18535-18545.	5.6	57
30	Efficient all-air processed mixed cation carbon-based perovskite solar cells with ultra-high stability. Journal of Materials Chemistry A, 2019, 7, 17594-17603.	10.3	56
31	Stable hybrid perovskite MAPb(I1â^'Br)3 for photocatalytic hydrogen evolution. Applied Catalysis B: Environmental, 2019, 253, 41-48.	20.2	56
32	Uniformly assembling n-type metal oxide nanostructures (TiO2 nanoparticles and SnO2 nanowires) onto P doped g-C3N4 nanosheets for efficient photocatalytic water splitting. Applied Catalysis B: Environmental, 2020, 278, 119301.	20.2	55
33	Dual-functional ZnO nanorod aggregates as scattering layer in the photoanode for dye-sensitized solar cells. Chemical Communications, 2011, 47, 11519.	4.1	49
34	Low Temperatureâ€Processed Stable and Efficient Carbonâ€Based CsPbI ₂ Br Planar Perovskite Solar Cells by In Situ Passivating Grain Boundary and Trap Density. Solar Rrl, 2019, 3, 1900109.	5.8	46
35	High crystallization of a multiple cation perovskite absorber for low-temperature stable ZnO solar cells with high-efficiency of over 20%. Nanoscale, 2018, 10, 7218-7227.	5.6	45
36	Assembled alginate/chitosan micro-shells for removal of organic pollutants. Polymer, 2009, 50, 2841-2846.	3.8	44

#	Article	IF	CITATIONS
37	Multidimensional ZnO Architecture for Dye‧ensitized Solar Cells with Highâ€Efficiency up to 7.35%. Advanced Energy Materials, 2014, 4, 1301802.	19.5	41
38	In situ assembly of well-defined Au nanoparticles in TiO2 films for plasmon-enhanced quantum dot sensitized solar cells. Nano Energy, 2018, 44, 135-143.	16.0	41
39	Formulation and cytotoxicity of doxorubicin loaded in self-assembled bio-polyelectrolyte microshells. International Journal of Pharmaceutics, 2007, 336, 376-381.	5.2	40
40	Low-Temperature Processing All-Inorganic Carbon-Based Perovskite Solar Cells up to 11.78% Efficiency via Alkali Hydroxides Interfacial Engineering. ACS Applied Energy Materials, 2020, 3, 401-410.	5.1	40
41	Broadband dye-sensitized upconverting nanocrystals enabled near-infrared planar perovskite solar cells. Journal of Power Sources, 2017, 372, 125-133.	7.8	38
42	Poly(amidoamine) dendrimer-grafted porous hollow silica nanoparticles for enhanced intracellular photodynamic therapy. Acta Biomaterialia, 2013, 9, 6431-6438.	8.3	36
43	Au-nanorod-anchored {0 0 1} facets of Bi4Ti3O12 nanosheets for enhanced visible-light-driven photocatalysis. Applied Surface Science, 2018, 448, 41-49.	6.1	36
44	Borate and iron hydroxide co-modified BiVO4 photoanodes for high-performance photoelectrochemical water oxidation. Chemical Engineering Journal, 2021, 421, 129819.	12.7	36
45	Rose Bengalâ€Grafted Biodegradable Microcapsules: Singletâ€Oxygen Generation and Cancer ell Incapacitation. Chemistry - A European Journal, 2011, 17, 11223-11229.	3.3	35
46	Efficient ambient-air-stable HTM-free carbon-based perovskite solar cells with hybrid 2D–3D lead halide photoabsorbers. Journal of Materials Chemistry A, 2018, 6, 22626-22635.	10.3	31
47	Preparation and characterization of PSâ€PMMA/ZnO nanocomposite films with novel properties of high transparency and UVâ€shielding capacity. Journal of Applied Polymer Science, 2010, 118, 1507-1512.	2.6	30
48	Hexamethylenetetramine-mediated growth of grain-boundary-passivation CH 3 NH 3 PbI 3 for highly reproducible and stable perovskite solar cells. Journal of Power Sources, 2018, 377, 103-109.	7.8	30
49	Silica Nanotubes Based on Needle-like Calcium Carbonate:Â Fabrication and Immobilization for Glucose Oxidase. Industrial & Engineering Chemistry Research, 2007, 46, 459-463.	3.7	29
50	Solution-processed electron transport layer of n-doped fullerene for efficient and stable all carbon based perovskite solar cells. Journal of Materials Chemistry A, 2019, 7, 7710-7716.	10.3	29
51	All room-temperature processing efficient planar carbon-based perovskite solar cells. Journal of Power Sources, 2021, 489, 229345.	7.8	29
52	A novel route for waste water treatment: photo-assisted Fenton degradation of dye pollutants accumulated in natural polyelectrolyte microshells. Chemical Communications, 2005, , 4607.	4.1	28
53	Fine control of perovskite-layered morphology and composition via sequential deposition crystallization process towards improved perovskite solar cells. Journal of Power Sources, 2016, 311, 130-136.	7.8	25
54	Efficient and long-term photocatalytic H2 evolution stability enabled by Cs2AgBiBr6/MoS2 in aqueous HBr solution. International Journal of Hydrogen Energy, 2022, 47, 8829-8840.	7.1	25

#	Article	IF	CITATIONS
55	A comparative study on indoline dye- and ruthenium complex-sensitized hierarchically structured ZnO solar cells. Electrochemistry Communications, 2012, 16, 57-60.	4.7	21
56	Plasmonic enhancement of light-harvesting efficiency in tandem dye-sensitized solar cells using multiplexed gold core/silica shell nanorods. Journal of Power Sources, 2018, 376, 26-32.	7.8	20
57	Assembling photosensitive capsules by phthalocyanines and polyelectrolytes for photodynamic therapy. Polymer, 2011, 52, 1766-1771.	3.8	19
58	Efficient charge separation promoting visible-light-driven photocatalytic activity of MnO x decorated WS 2 hybrid nanosheets. Electrochemistry Communications, 2016, 72, 118-121.	4.7	19
59	Dual functions of heterometallic FeCo oxyhydroxides in borate-treated BiVO4 photoanodes toward boosted activity and photostability in photoelectrochemical water oxidation. Chemical Engineering Journal, 2022, 431, 133379.	12.7	19
60	Enhanced Visible-Light Photoelectrocatalytic Degradation of Organic Contaminants at Iodine-Doped Titanium Dioxide Film Electrode. Industrial & Engineering Chemistry Research, 2012, 51, 218-224.	3.7	16
61	Enhanced performance of dye-sensitized solar cells via the incorporation of an internal layer consisting of three-dimensional shuttlelike up-converter and ZnO nanocrystalline aggregates. Journal of Power Sources, 2013, 243, 588-593.	7.8	16
62	Morphology inheritance synthesis of carbon-coated Li3VO4 rods as anode for lithium-ion battery. Science China Materials, 2019, 62, 1105-1114.	6.3	16
63	Storage and sustained release of volatile substances from a hollow silica matrix. Nanotechnology, 2007, 18, 245705.	2.6	15
64	Enhanced Photosensitized Degradation of Organic Pollutants under Visible Radiation by (I ₂) _n -Encapsulated TiO ₂ Films. Industrial & Engineering Chemistry Research, 2012, 51, 1110-1117.	3.7	15
65	Ethylenediamine chlorides additive assisting formation of high-quality formamidinium-caesium perovskite film with low trap density for efficient solar cells. Journal of Power Sources, 2020, 449, 227484.	7.8	14
66	Ultra-low-cost all-air processed carbon-based perovskite solar cells from bottom electrode to counter electrode. Journal of Power Sources, 2020, 478, 228764.	7.8	14
67	Facile encapsulation of nanoparticles in nanoorganized bio-polyelectrolyte microshells. Polymer, 2007, 48, 7598-7603.	3.8	13
68	Stable and efficient Ti3C2 MXene/MAPbI3-HI system for visible-light-driven photocatalytic HI splitting. Journal of Power Sources, 2022, 522, 231006.	7.8	13
69	Visible light-driven binary dyes synergic degradation by iodine-doped TiO2 nanocrystal film. Catalysis Communications, 2012, 20, 94-98.	3.3	12
70	Coreâ€Shell Structured Biâ€Amorphous SiO ₂ @TiO ₂ Composite for Lithiumâ€Ion Batteries Anode Material with Ultraâ€Stable Performance. ChemistrySelect, 2020, 5, 5198-5204.	1.5	12
71	Stable Mixed-Organic-Cation Perovskite MA _{1–<i>x</i>} FA _{<i>x</i>} PbI ₃ Integrated with MoS ₂ for Enhanced Visible-Light Photocatalytic H ₂ Evolution. Industrial & Engineering Chemistry Research. 2020. 59. 20667-20675.	3.7	12
72	Photooxidative Degradation of Dye Pollutants Accumulated in Self-Assembled Natural Polyelectrolyte Microshells under Visible Radiation. Chemistry - A European Journal, 2006, 12, 4164-4169.	3.3	11

#	Article	IF	CITATIONS
73	Pseudo metallic (1T) molybdenum disulfide for efficient photo/electrocatalytic water splitting. Applied Catalysis B: Environmental, 2022, 307, 121156.	20.2	11
74	Functionalization of ZnO aggregate films via iodine-doping and TiO ₂ decorating for enhanced visible-light-driven photocatalytic activity and stability. RSC Advances, 2016, 6, 24430-24437.	3.6	10
75	An Efficient and Extremely Stable Photocatalytic PtSe ₂ /FTO Thin Film for Water Splitting. Energy Technology, 2020, 8, 1900903.	3.8	10
76	Promoting photocatalytic degradation of tetracycline over in-situ grown single manganese atoms on polymeric carbon nitride. Applied Surface Science, 2022, 593, 153458.	6.1	10
77	In-Situ Hydrothermal Growth of Bi-Hierarchical ZnO Nanoarchitecture with Surface Modification for Efficient Hybrid Solar Cells. Electrochimica Acta, 2014, 145, 116-122.	5.2	9
78	Visible-light driven C@TiO2 porous films: Enhanced photoelectrochemical and photoelectrocatalytic performance. Catalysis Communications, 2015, 69, 63-67.	3.3	9
79	A facile and broadly applicable CdBr ₂ -passivating strategy for halide migration-inhibiting perovskite films and high-performance solar cells. Journal of Materials Chemistry A, 2021, 9, 14758-14767.	10.3	9
80	A gel-state dye-sensitized hierarchically structured ZnO solar cell: Retention of power conversion efficiency and durability. Electrochimica Acta, 2013, 114, 700-705.	5.2	8
81	Bromide Induced Roomâ€Temperature Formation of Photoactive Formamidiniumâ€Based Perovskite for Highâ€Efficiency, Lowâ€Cost Solar Cells. Solar Rrl, 2019, 3, 1800313.	5.8	7
82	Composition Engineering–Triggered Bifunctionality of Freeâ€6tanding Coralâ€Like 1Tâ€MoS ₂ for Highly Efficient Overall Water Splitting. Energy Technology, 2020, 8, 2000268.	3.8	7
83	Effects of precursor concentration and annealing temperature on CH 3 NH 3 PbI 3 film crystallization and photovoltaic performance. Journal of Physics and Chemistry of Solids, 2017, 107, 55-61.	4.0	6
84	Micron-scale ultrathin two-dimension zirconia nanosheets towards enhancing anticorrosion performance of epoxy coatings. Tungsten, 2021, 3, 459-469.	4.8	6
85	Au nanoparticle homogeneously decorated C@TiO ₂ for enhanced visible-light-driven photocatalytic activity. RSC Advances, 2015, 5, 103790-103796.	3.6	5
86	A Costâ€Effective and Scaleable Approach for the Inâ€Situ Synthesis of Porous Carbonâ€Coated Micrometerâ€Sized AlSi Particles as Anode for Lithiumâ€Ion Batteries. ChemElectroChem, 2019, 6, 2517-2523.	3.4	4
87	NH ₄ Brâ€Assisted Two‣tepâ€Processing of Guanidiniumâ€Rich Perovskite Films for Extremely Stable Carbonâ€Based Perovskite Solar Cells in Ambient Air. Solar Rrl, 0, , 2101103.	5.8	4
88	Polyvinylpyrrolidoneâ€Mediated In Situ Synthesis of Wellâ€Connected Ni 3 V 2 O 8 /C Nanocomposite Anode for Lithiumâ€ion Batteries. Energy Technology, 2020, 8, 1901461.	3.8	3
89	Hybrid rinse solvent processing highly flat perovskite films on planar substrate. Electrochemistry Communications, 2018, 91, 71-74.	4.7	2
90	NH ₄ Brâ€Assisted Two‣tepâ€Processing of Guanidiniumâ€Rich Perovskite Films for Extremely Stable Carbonâ€Based Perovskite Solar Cells in Ambient Air. Solar Rrl, 2022, 6, .	5.8	2

#	Article	IF	CITATIONS
91	Bromide Induced Roomâ€Temperature Formation of Photoactive Formamidiniumâ€Based Perovskite for Highâ€Efficiency, Lowâ€Cost Solar Cells (Solar RRL 4â^•2019). Solar Rrl, 2019, 3, 1970045.	5.8	Ο